

THE DESIGN AND ANALYSIS OF A ROTARY MOTION ELECTROSTATIC ACTUATOR

TAN AIK CHOON

**A report submitted in partial fulfilment of the requirements for the degree of
Mechatronics Engineering**



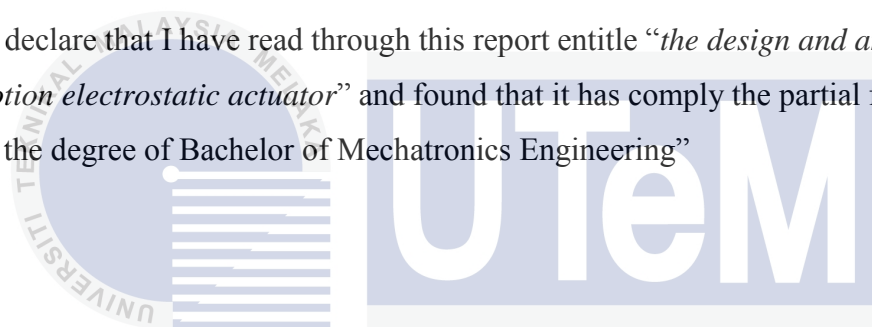
Faculty of Electrical Engineering

UNIVERSITI TEKNIKAL MALAYSIA MELAKA

2014

SUPERVISOR'S ENDORSEMENT

"I hereby declare that I have read through this report entitle "*the design and analysis of a rotary motion electrostatic actuator*" and found that it has comply the partial fulfilment for awarding the degree of Bachelor of Mechatronics Engineering"



Signature :
اونيورسي تيكنيكل مليسيا ملاك

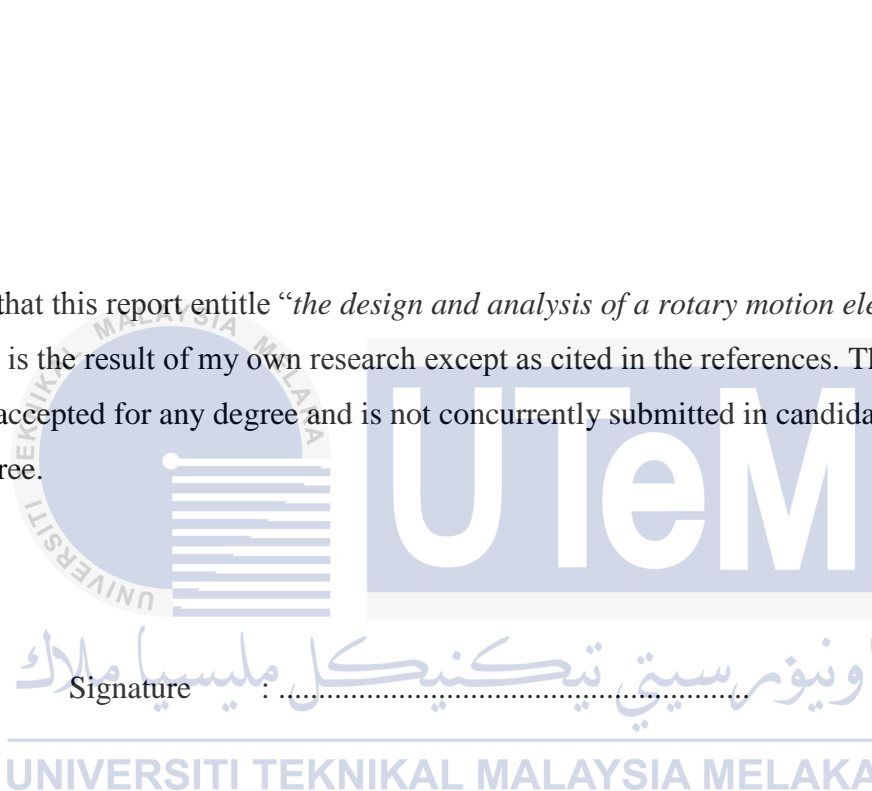
UNIVERSITI TEKNIKAL MALAYSIA MELAKA

Supervisor's Name : Dr. Mariam Md Ghazaly

Date :

STUDENT DECLARATION

I declare that this report entitle “*the design and analysis of a rotary motion electrostatic actuator*” is the result of my own research except as cited in the references. The report has not been accepted for any degree and is not concurrently submitted in candidature of any other degree.



Name : Tan Aik Choon

Date :

ACKNOWLEDGEMENT

The special thank goes to my helpful supervisor, Dr. Mariam Md Ghazaly. The supervision and support that she gave truly help the progression and smoothness of the final year project.

My grateful thanks also go to the technicians and master students that help me from time to time during this project. All the outcomes during this period would be nothing if without the enthusiasm of them.

Last but not least, great deals appreciated go to the contribution of my faculty- Faculty of Electrical Engineering and our university- Universiti Teknikal Malaysia Melaka for providing us facilities and equipment to convenience us in our final year project.



ABSTRACT

Research and development in microelectromechanical systems (MEMS) or most generally defined as miniaturized electromechanical elements, have made outstanding progress. MEMS consist of micromechanisms such as microstructures, microactuators, microsensors and their control circuits. There are two types of microactuator used in MEMS which are linear motion and rotary motion. Both types of actuator consist of electromagnetic, electrostatic, thermal, shape-memory alloy and others. Each type of actuator has its own advantages and drawbacks. This report provides a brief comparison of those actuators and overview of the design of two types of rotary motion electrostatic actuator. It focuses on the thrust force produced when different parameters are manipulated for both designs. Both designs are set to have the same size which is 1.4mm in diameter and thickness is 50 μm ; both designs have the same number of electrode for stator and rotor too which are twelve electrodes and sixteen electrodes respectively. To analyse the thrust force produce, Ansys, Maxwell3D is used as a tool to design and analyse the two rotary motion electrostatic actuators. Three simulations have been carried out; first, vary the actuator size; second, vary the actuator thickness; third, vary the number of electrode. With the same rotor size, thickness, gap, and number of electrode, the results show that bottom-drive electrostatic actuator has better performance than side-drive electrostatic actuator through simulation.

ABSTRAK

Penyelidikan dan pembangunan dalam sistem mikroeletromekanik (MEMS) atau paling umumnya didefinisikan sebagai elemen elektromekanik bersaiz kecil, telah mencapai kemajuan yang menakjubkan. MEMS terdiri daripada mekanisme mikro seperti struktur mikro, penggerak mikro, sensor mikro dan litar kawalan mereka. Terdapat dua jenis penggerak mikro digunakan dalam MEMS iaitu gerakan linear dan gerakan berputar. Kedua-dua jenis penggerak terdiri daripada elektromagnetik, elektrostatik, haba, aloi bentuk-memori dan lain-lain. Setiap jenis penggerak mempunyai kelebihan dan kelemahan sendiri. Laporan ini memberi perbandingan yang ringkas dari penggerak yang telah dinyatakan dan gambaran tentang reka bentuk dua jenis penggerak berputar elektrostatik. Laporan ini memberi tumpuan kepada kekuatan yang dihasil apabila parameter yang berbeza dimanipulasi. Kedua-dua reka bentuk mempunyai saiz yang sama iaitu 1.4mm diameter dan ketebalan 50 μ m; kedua-dua reka bentuk mempunyai jumlah elektrod yang sama bagi pemegun dan pemutar iaitu dua belas elektrod dan enam belas elektrod masing-masing. Untuk menganalisis hasil daya tujahan, ANSYS Maxwell3D digunakan sebagai alat untuk mereka bentuk dan menganalisis dua penggerak berputar elektrostatik. Tiga simulasi telah dijalankan; pertama, mengubah saiz penggerak; kedua, mengubah ketebalan penggerak; ketiga, mengubah bilangan elektrod. Dengan saiz pemutar, ketebalan, jurang, dan bilangan elektrod yang sama, keputusan menunjukkan bahawa penggerak elektrostatik *bottom-drive* mempunyai pretasi yang lebih baik daripada penggerak elektrostatik *side-drive* secara teori.

TABLE OF CONTENTS

TITLE	PAGE
ACKNOWLEDGEMENT	i
ABSTRACT	ii
ABSTRAK.....	iii
TABLE OF CONTENTS	iv
LIST OF TABLES.....	vi
LIST OF FIGURES.....	vii
LIST OF APPENDICES.....	ix
INTRODUCTION.....	1
1.1 Motivation.....	1
1.2 Problem Statement.....	1
1.3 Objectives	2
1.4 Scopes	2
1.5 Thesis Overview	3
LITERATURE REVIEW	4
2.1 Electric Machines	4
2.2 Actuation Systems	4

METHODOLOGY	9
3.1 Basic Actuation Principle	9
3.2 Working Principle of Electrostatic Actuator.....	10
3.3 Design structure	11
3.3.1 Design 1 (side-drive electrostatic actuator)	12
3.3.2 Design 2 (bottom-drive electrostatic actuator)	13
3.4 Procedure	14
3.5 Simulation.....	17
3.5.1 Vary actuator size	17
3.5.2 Vary actuator thickness	18
3.5.3 Vary the teeth number of stator and rotor.....	19
RESULT & DISCUSSION	21
4.1 Preliminary Results.....	21
4.1.1 Effect of electrode width and voltage on electrostatic force	21
4.1.2 Effect of gap and voltage on electrostatic force	26
4.1.3 Effect of electrode width and gap on electrostatic force	31
4.2 Simulation results	35
4.2.1 Effect of actuator size on electrostatic force	35
4.2.2 Effect of actuator thickness on electrostatic force.....	38
4.2.3 Effect of teeth number on electrostatic force.....	41
CONCLUSION	44
REFERENCES	45
APPENDIX	458

LIST OF TABLES

TABLE	TITLE	PAGE
Table 2.1:	Actuator models	5
Table 2.2:	Comparison of different actuators in different drive types [19].....	7
Table 2.3:	Characteristics of various microactuator types [8].....	7
Table 3.1:	Design parameters of both designs.....	14
Table 4.1:	Force of Design 1 by manipulating the electrode width and voltage.....	22
Table 4.2:	Force of Design 2 by manipulating the width and voltage	24
Table 4.3:	Force of Design 1 by manipulating gap and voltage.....	27
Table 4.4:	Force of Design 2 by manipulating gap and voltage.....	29
Table 4.5:	Force of Design 1 by manipulating gap and electrode width.....	31
Table 4.6:	Force of Design 2 by manipulating width and distance	33
Table 4.7:	The best parameter for Design 1 and Design 2	35
Table 4.8:	Electrostatic force by varying side-drive actuator size	35
Table 4.9:	Electrostatic force by varying bottom-drive actuator size.....	37
Table 4.10:	Electrostatic force by varying side-drive actuator thickness.....	39
Table 4.11:	Electrostatic force by varying bottom-drive actuator thickness.....	40
Table 4.12:	Electrostatic force produced by varying teeth ratio of side-drive actuator	41
Table 4.13:	Electrostatic force produced by varying teeth ratio of bottom-drive actuator ..	42

LIST OF FIGURES

FIGURE	TITLE	PAGE
Figure 3.1:	Lateral electrostatic force on parallel plate	9
Figure 3.2:	Working principle of the three-phase electrostatic rotary stepper motor.....	11
Figure 3.3:	Side-drive electrostatic actuator (Design 1).....	12
Figure 3.4:	Dimensions for Design 1	12
Figure 3.5:	Bottom-drive electrostatic actuator (Design 2).....	13
Figure 3.6:	Dimensions for Design 2	13
Figure 3.4:	Layout of Maxwell 3D.....	15
Figure 3.5:	Size of side-drive actuator vary from 700 μm to 100 μm	18
Figure 3.6:	Size of bottom-drive actuator vary from 700 μm to 100 μm	18
Figure 3.7:	Thickness of side-drive actuator vary from 50 μm to 10 μm	19
Figure 3.8:	Thickness of bottom-drive actuator vary from 50 μm to 10 μm	19
Figure 3.9:	Teeth ratio of side-drive actuator vary from 12:9 to 28:21.....	20
Figure 3.10:	Teeth ratio of bottom-drive actuator vary from 12:9 to 28:21.....	20
Figure 4.1:	Force of Design 1 by manipulating electrode width and voltage	23
Figure 4.2:	Force of Design 2 by manipulating electrode width and voltage	26
Figure 4.3:	Force of Design 1 by manipulating gap and voltage	28
Figure 4.4:	Force of Design 2 by manipulating gap and voltage	30
Figure 4.5:	Force of Design 1 by manipulating electrode width and gap	32
Figure 4.6:	Force of Design 2 by manipulating width and distance.....	34
Figure 4.7:	Electrostatic force produced with different side-drive actuator size.....	36
Figure 4.8:	Electrostatic force produced with different bottom-drive actuator size.....	38
Figure 4.9:	Electrostatic force produced with different side-drive actuator thickness.....	39
Figure 4.10:	Electrostatic force produced with different bottom-drive actuator thickness.	40
Figure 4.11:	Electrostatic force produced with different side-drive actuator teeth number.	42

Figure 4.12: Electrostatic force produced with different bottom-drive actuator teeth number.

..... 43



LIST OF APPENDICES

APPENDIX	TITLE	PAGE
A	Gantt chart	45



CHAPTER 1

INTRODUCTION

1.1 Motivation

Microactuator is a subset of microelectromechanical systems (MEMS) that convert electrical energy to mechanical energy. With advance technologies in microfabrication for MEMS, an efficient and reliable microactuator can be built for various microsystems such as mobile microrobots. Microactuators can be used for development in biotechnology, medicine, communication, inertial sensing and so on. In medicine, microactuators are used for developing microsurgery instruments [1, 2], for example cutters, endoscopes [3] and graspers.

The motivation for this project is to analyse and optimize the best rotary electrostatic actuator for the realization of ideal microsystems and become the best solution for more and more applications.

1.2 Problem Statement

The growth of interest in Micro Electro Mechanical System (MEMS) is rapid nowadays. MEMS consist of micromechanisms such as microstructures, microactuators, microsensors and their control circuits. Types of microactuator used in MEMS include electrostatic, electromagnetic, piezoelectric, shape memory-alloy and so on. Although

electromagnetic actuator is widely used in industry, but when in small size scales, electrostatic actuator has the advantages. The fabrication of the electrostatic actuator is simpler than electromagnetic actuator. On the micro scale, the energy densities of electrostatic and electromagnetic actuators are comparable. Therefore, from the performance point of view, the micro scale electrostatic actuators are comparable to the electromagnetic actuators and in particular cases the electrostatic actuators may be better.

1.3 Objectives

The aim of this thesis is the generation of electrostatic force between two different types of rotary motion electrostatic actuator. Therefore, the objectives of this thesis are set as below:

1. To design two types of rotary motion electrostatic actuator.
2. To analyse and optimize the performances of both electrostatic actuator designs in different parameters.

1.4 Scopes

The central focus of this thesis is to figure out which types of rotary motion electrostatic actuator produce the greatest thrust force using Finite Element Method (FEM). To achieve the aim, the task is divided into three main parts:

1. Design two types of rotary motion electrostatic actuator; side-drive electrostatic actuator and bottom-drive electrostatic actuator.
2. Analyse the thrust force and working range of these two designs by using FEM.
3. Optimize the thrust force and working range for both designs by manipulating the size of actuator, actuator thickness, and the number of electrode with FEM.

1.5 Thesis Overview

This thesis is categorized into five chapters as listed below. The main body of work is included in Chapter 3 and 4, continued by conclusion in Chapter 5.

Chapter 1: The motivation and problem statement of this research are stated which inspired this research issue. In addition, the objectives and scopes of this research are also included.

Chapter 2: This chapter shows the information found in the literature that related to this research. The review of those literatures is evaluated, managed, explained, and summerized. An assessment is then written.

Chapter 3: The mathematical theory of electrostatic force is discussed followed by the working principle of electrostatic actuator and the design structure for two different types of rotary motion electrostatic actuator.

Chapter 4: The simulation results for both side-drive electrostatic actuator and bottom-drive electrostatic actuator are shown in this chapter and the results are discussed.

Chapter 5: This chapter states the summary, relavant conclusions, and some further research of this thesis.

CHAPTER 2

LITERATURE REVIEW

2.1 Electric Machines

Electric machines are the equipment that converts electrical energy to mechanical energy in rotary motion or linear motion. According to Trimmer and Gabriel, Gordon and Franklin built the first electrostatic motors in 1750s, 100 years before magnetic motors [4]. The first capacitive electrostatic motor was developed during Edison's era in 1889 by Zipernowsky [5].

Several types of microactuators have been studied widely such as electromagnetic, piezoelectric, electrostatic, and so on; Table 2.1 shows the working principle of those microactuators that are widely used in industry while Table 2.2 shows the comparison for the drive type of those microactuators.

The operating principle of variable-capacitance is synchronous machines that produce torque due to spatial misalignment of electrodes on the stator and salient poles on the rotor. Trimmer and Gabriel proposed the concept of linear and rotary variable-capacitance micromotors in 1987 [4].

2.2 Actuation Systems

A brief description will be given for each of the classes of actuators and the detail operating principles is shown in Table 2.1.

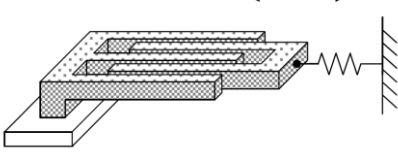
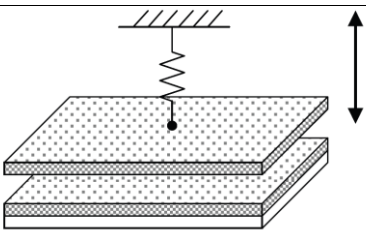
Piezoelectric actuator: The materials of piezoelectric will strain when external electric field is applied. Therefore electric field levels are always limited to a lower value to avoid electrical and mechanical fatigue.

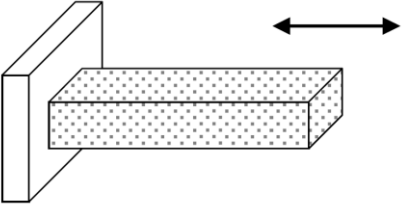

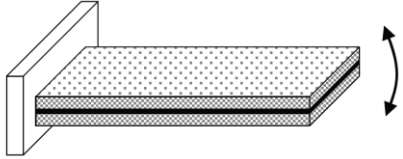
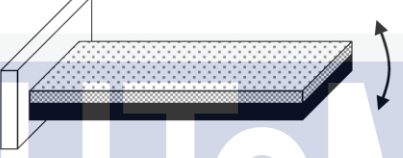
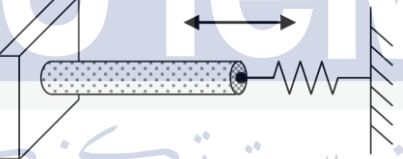


Shape memory alloy actuator: Shape memory alloys are mostly used in form of foil or wire. When shape memory alloys get heated, the length will be reduced; and will back to original length when cooled.

Thermal expansion actuator: The actuation principle for thermal expansion actuator is the opposite way of shape memory alloy actuator. Thermal expansion actuator expands its length when heated and can withstand temperature up to 100 K.

Electromagnetic actuator: Electromagnetic actuator can be divided into three forms: solenoids, moving coil transducers, and motors. Solenoids consist of a high permeability rod and an electromagnetic coil; when the coil is energized, the magnetic field generated will pull the rod. The actuation principle for moving coil transducers are almost the same with solenoid, the only difference is the moving part is the coil while the rod remains stationary. By using the same principle, motors can produce infinite range of displacements.

Table 2.1: Actuator models

	Actuator	Geometry	Operating Principle
Electrostatic	Comb drive [11]		Electrostatic force
	Parallel plate [12]		

Thermal	Thermal expansion [13]		Thermal expansion
	Thermal bimaterial cantilever [14]		
Piezoelectric	Piezoelectric bimorph [15]		Converse piezoelectric effect
	Piezoelectric unimorph [15]		
Shape Memory Alloy (SMA)	SMA wire [16]		Thermally induced phase change
	SMA biomaterial cantilever [17]		
	Dielectric elastomer [18]		

After summarizing the actuation principles of different actuator types, the drive range, speed, and response are then compared between linear motion and rotary motion in Table 2.2. From Table 2.2, rotary motion electrostatic actuator has better performances compared with other actuators.

Table 2.2: Comparison of different actuators in different drive types [19]

	Drive type	Drive range	Speed	Response
Electrostatic	Linear	Small	Low	High
	Rotary	Large	High	Medium to high
Piezoelectric	Linear	Small	Low	High
	Rotary	Large	Low to medium	Low to medium
Electromagnetic	Linear	Small to medium	Low to medium	High
	Rotary	Large	Medium to high	Medium to high

In Table 2.3, electrostatic actuator and others actuator are compared from several aspects: maximum deflection, maximum force, speed of actuation and efficiency. The result shows that electrostatic actuator has the minimum deflection, highest speed of actuation, and the highest efficiency.

UNIVERSITI TEKNIKAL MALAYSIA MELAKA

Table 2.3: Characteristics of various microactuator types [8]

Actuator	Maximum Deflection	Maximum Force	Speed of Actuation	Efficiency (%)
Electrostatic	Low	Low	Very Fast	>90
Piezoelectric	High	Medium	Fast	10-30
Thermal	Medium	Very High	Slow	<5
Shape Memory Alloy	High	Very High	Slow	<5

After a series of comparative studies are presented, it is shown that rotary motion electrostatic actuators have better performance because they can be operated in very high speeds, precise in positioning, large working range and have repeatable movement. However, those research only focus on experimental result of the fabricated electrostatic actuator; therefore this thesis is aim to compare the simulation results of side-drive electrostatic actuator and bottom-drive electrostatic actuator and analyse which drive type of actuator give the better performance.



CHAPTER 3

METHODOLOGY

3.1 Basic Actuation Principle

A fundamental property of electrons and protons is charge. Charged particles can be either positively or negatively charged, and experiments show that same charges repel while different charges attract. The magnitude of the force between the particles is depends on the medium in which the charges are located, and this is taken into account by the factor ε which is known as the permittivity of the medium. The permittivity of a medium is $\varepsilon = \varepsilon_r \varepsilon_0$ where ε_0 is a fundamental constant known as the vacuum permittivity which has the value $8.854 \times 10^{-12} \text{ J}^{-1} \text{ C}^2 \text{ m}^{-1}$ and ε_r is the relative permittivity of the medium. [6, 7]

The tangential force F exerted on rotor poles can be estimated using the parallel plate capacitor formula [10]. When a voltage difference is applies between two parallel plates, an alignment force F is produced as shown in Figure 3.1.

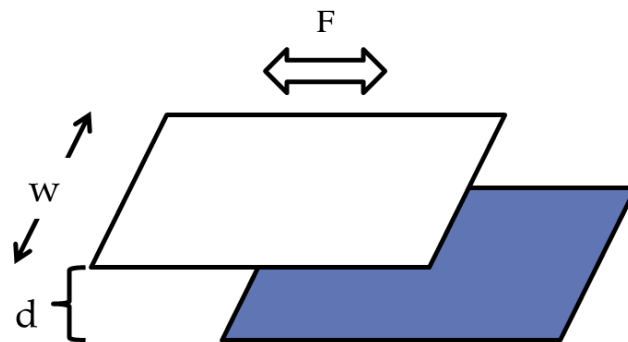


Figure 3.1: Lateral electrostatic force on parallel plate

$$F = n \frac{1}{2} \epsilon_0 \frac{w}{d} V^2 \quad (3.1)$$

Where,

n is the number of active poles in a phase

w is the width of the pole

d is the distance between the rotor and stator poles

ϵ_0 is the permittivity of air

V is the voltage applied

3.2 Working Principle of Electrostatic Actuator

Stepper microactuator consists of a grounded rotor and a 3-phase stator, both having a large number of teeth-like electrodes. During operation, the rotor electrodes are grounded and the stator electrodes are grouped in three different electrical phases that are symmetrically located around the rotor. Each phase can be activated independently. In the initial position, the electrodes of the first phase are perfectly aligned with the opposite electrodes on the rotor. By applying a voltage difference on one of the misaligned phases, an electrostatic force can be generated. By changing the phase sequences, either clockwise or counter-clockwise stepwise motion of the rotor can be achieved [9].

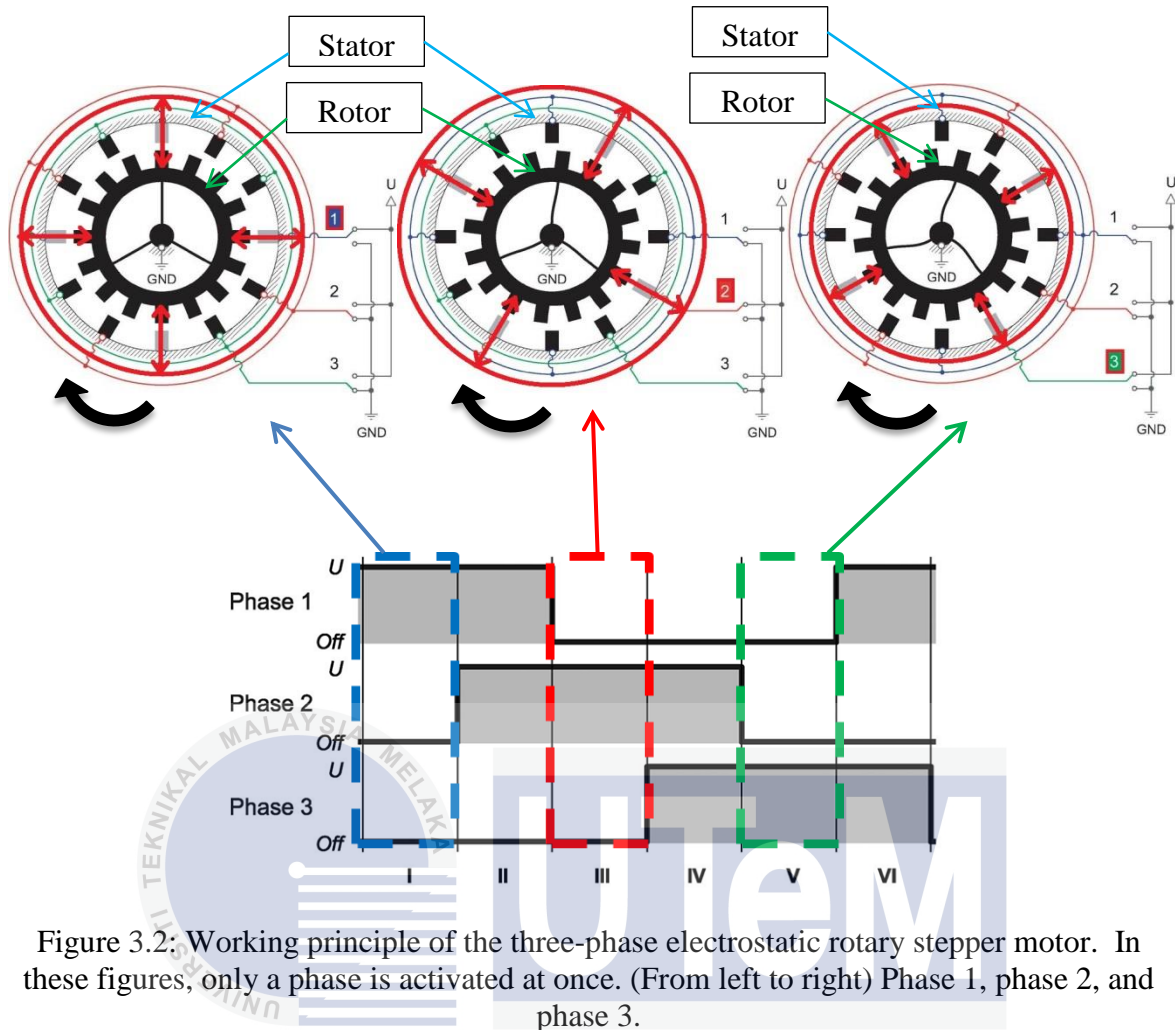


Figure 3.2: Working principle of the three-phase electrostatic rotary stepper motor. In these figures, only a phase is activated at once. (From left to right) Phase 1, phase 2, and phase 3.

3.3 Design structure

Figure 3.3 and Figure 3.5 show the three-dimensional view of two different electrostatic rotary motion actuators that having 12 stators and 16 poles rotor so that it will function as a three-phase motor. In the actuators shown in Figure 3.3 and Figure 3.5, the diameter of rotor is 1.4mm, and the gap between the stator and rotor is $2\mu\text{m}$ for both designs. The main dimensions of the designs are listed in Table 3.1. The operation of these actuators relies on the electrical energy stored in the variable capacitances formed between the poles of the rotor and the stator. The stator poles are connected in an alternative sequence with three electrical phases, each phase activates a group of stator independently. When a phase is activated, a voltage difference between the corresponding stator poles and the opposite rotor poles generates an electrostatic force. The electrostatic force tends to realign the poles of rotor with the activated stator poles.

3.3.1 Design 1 (side-drive electrostatic actuator)

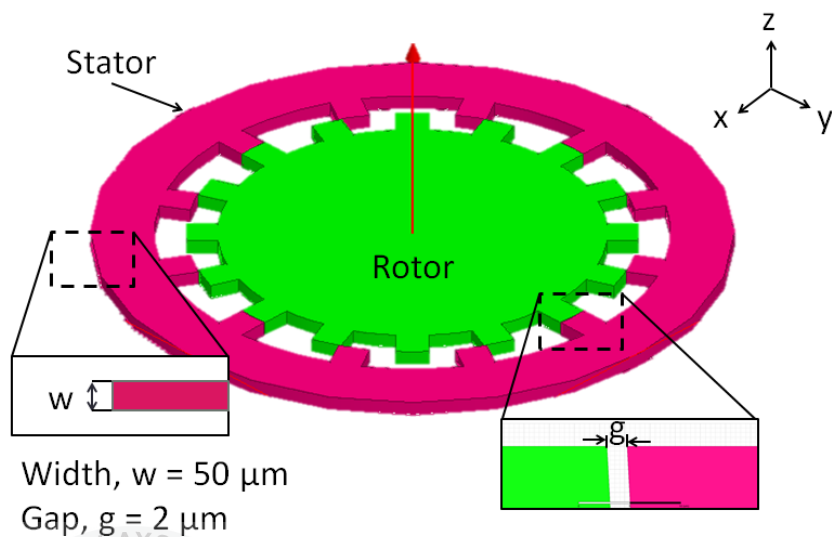


Figure 3.3: Side-drive electrostatic actuator (Design 1)

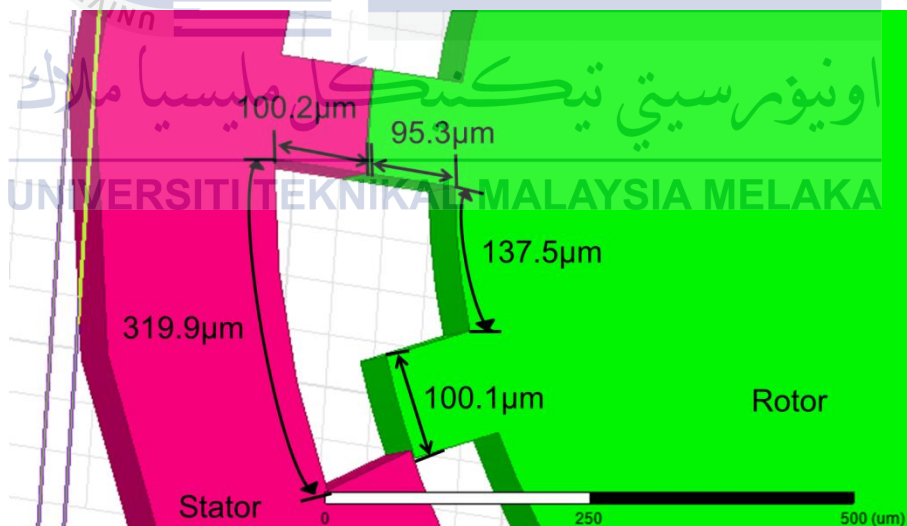


Figure 3.4: Dimensions for Design 1

3.3.2 Design 2 (bottom-drive electrostatic actuator)

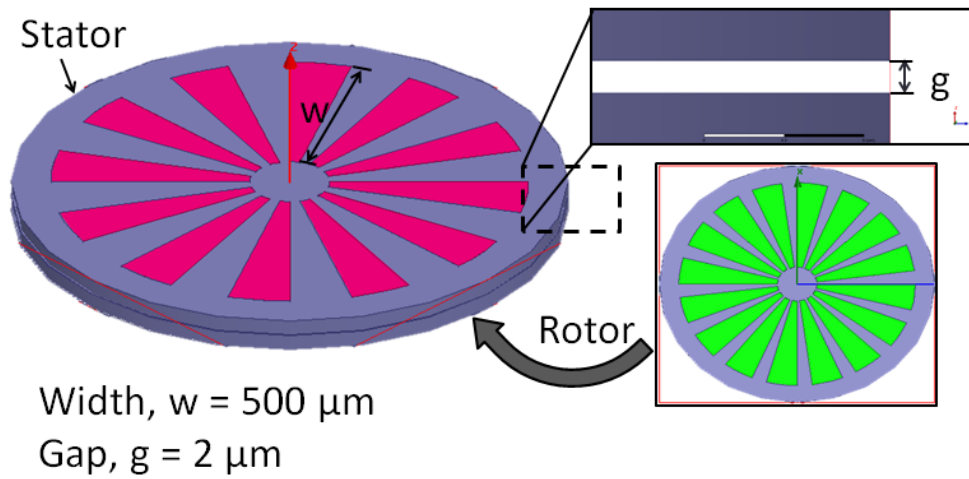


Figure 3.5: Bottom-drive electrostatic actuator (Design 2)

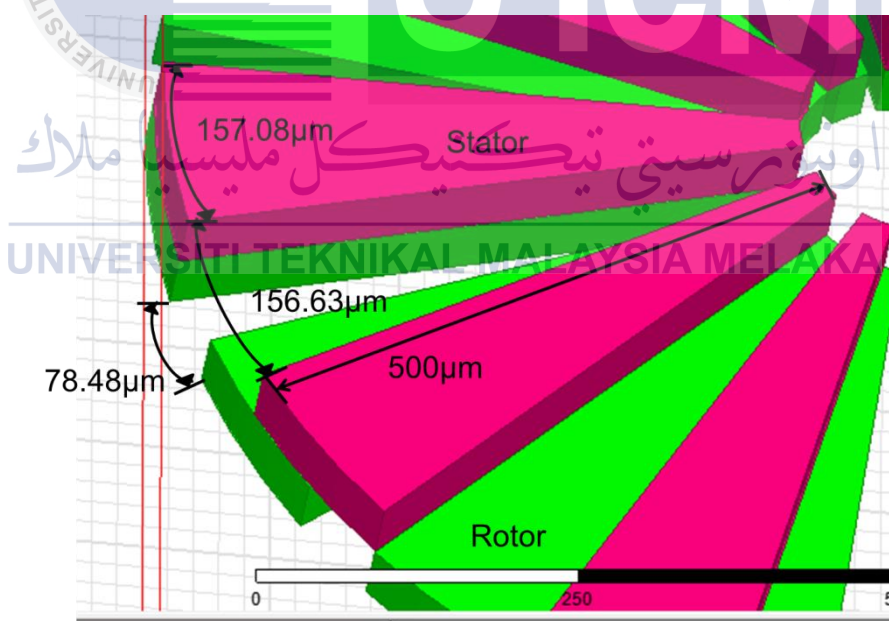


Figure 3.6: Dimensions for Design 2

Both structures are made of bronze, the gaps between stator and rotor are assumed filling with vacuum. Table 3.1 shows the design parameters of both side-drive and bottom-

drive electrostatic actuators. Generally, both actuators have the same size but different pole width due to different structure in design. Electrostatic force analysis was performed with different actuator size and thickness, the results are generated and computed.

Table 3.1: Design parameters of both designs

Parameter	Symbol	Value
Rotor radius	r	700 μm
Pole width (Design 1)	w_1	50 μm
Pole width (Design 2)	w_2	500 μm
Gap (rotor/stator)	d	2 μm
No. of active poles per phase	n	4

3.4 Procedure

In this project, ANSYS Maxwell 3D is used to simulate the electrostatic force of both designs by manipulating their parameters. Maxwell 3D is a high performance interactive software package that uses finite element analysis (FEA) to solve magnetic, electric, eddy current, and transient problems. Figure 3.4 shows the layout of the software.

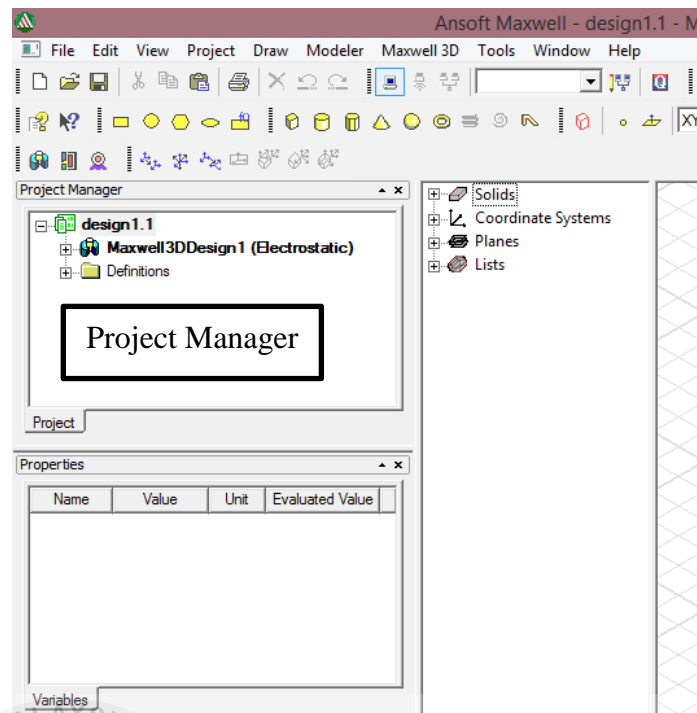


Figure 3.4: Layout of Maxwell 3D

1. Specify solution type

In Maxwell 3D, there are several solution types available. For the actuator of this report, *Electrostatic* solution is chosen. From the task bar:

Maxwell3D > Solution Type > Electrostatic

2. Set drawing units

Since the design of the actuator is small in size, therefore unit is set in micrometre. From the task bar:

Modeler > Units > μm

After all the setting is set, the design of actuator is started to draw. When the designs are completed, parameters are needed to add in.

3. Create background (Region)

A background has to be defined with a region box. To create a region box:

Draw > Region > Set all Evaluated Value to 300

4. Define material properties

Vacuum is automatically defined as the default material properties when geometry objects are created. To define the material for the actuator:

Double-click the actuator > From *Properties* window, in *Material* row, click the value in *Value* column > Select *Edit...* > Select *bronze* > Click *OK* to close the window

Leave the material assignment for *Region* unchanged.

5. Assign excitations

Voltages needed to be defined and assigned as excitations for rotor and stator of the actuator.

Select *stator* > Click *Maxwell3D > Excitations > Assign > Voltage > Type 100* in the *Value* box > Select *V* as the units > *OK*

Repeat steps to assign *0V* to *rotor* as grounded.

6. Set up force calculation

Select *rotor* > Click *Maxwell3D > Parameters > Assign > Force > Leave the Type set to Virtual > OK*

7. Set up analysis

To set up the analysis:

Right-click *Analysis* in *Project Manager* > Select *Add Solution Setup* > Click *General* tab in *Solve Setup* dialog box > Set *Maximum Number of Passes* = 10 and *Percent Error* = 5 > *OK*

These settings will instruct the solver to solve up to 10 passes as the automatic adaptive mesh refinement refines the mesh and improves the accuracy of the solution at run time.

8. Run the analysis

Right-click *Analysis* in *Project Manager* > Select *Analyze All*

3.5 Simulation

3.5.1 Vary actuator size

In the first simulation, size of both actuators is varied and the electrostatic force produced is recorded. The gap between stator and rotor, the teeth number, and the thickness of actuator are the fixed variables; the manipulated variables are size of actuator and voltage supplied. Figure 3.5 and Figure 3.6 show the actuators varied in different sizes.

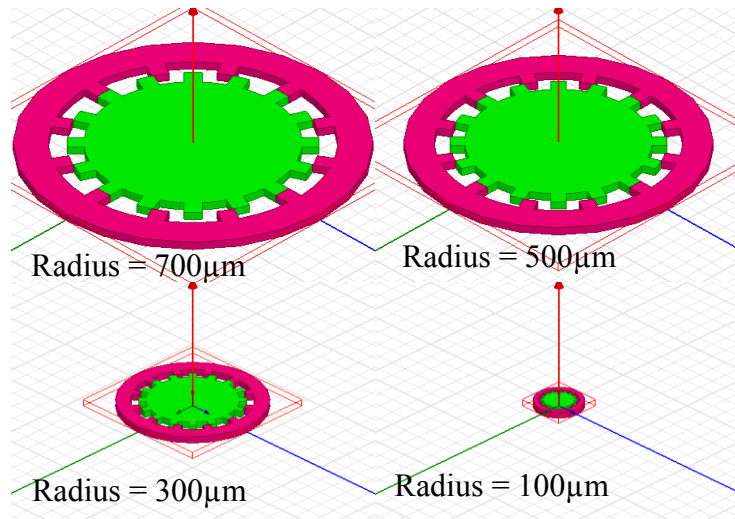


Figure 3.5: Size of side-drive actuator vary from 700 μm to 100 μm

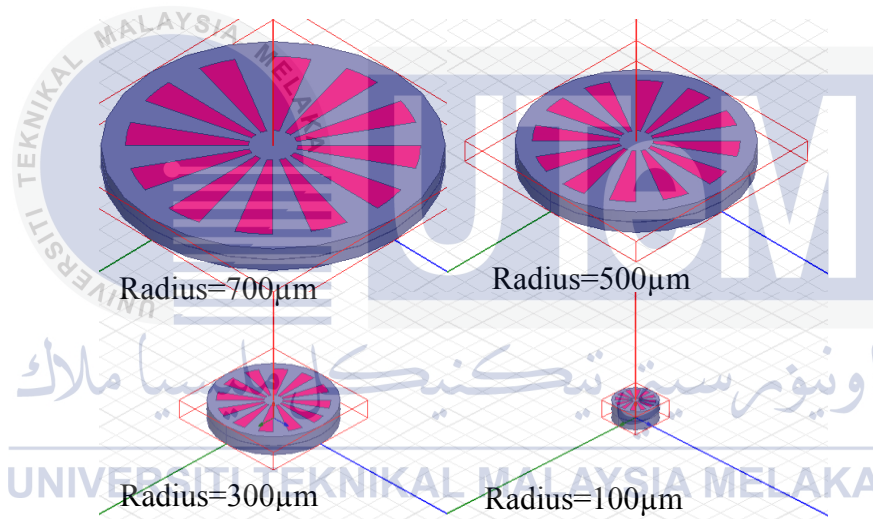


Figure 3.6: Size of bottom-drive actuator vary from 700 μm to 100 μm

3.5.2 Vary actuator thickness

In this simulation, thickness of both side-drive and bottom-drive actuator is varied and the electrostatic force is recorded. The fixed variables of this simulation are the size of actuator, the gap between stator and rotor, and the teeth number, the thickness of actuator and voltage supplied are the manipulated variables. Figure 3.7 and Figure 3.8 show the actuators varied in different thicknesses.

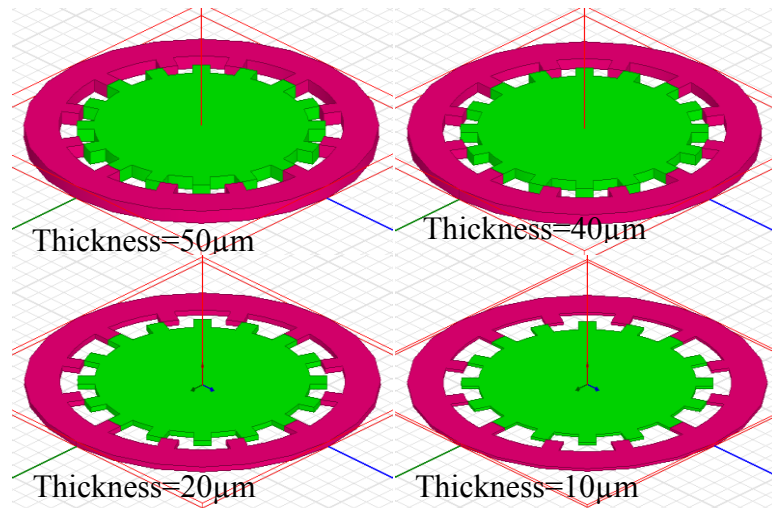


Figure 3.7: Thickness of side-drive actuator vary from 50 μm to 10 μm

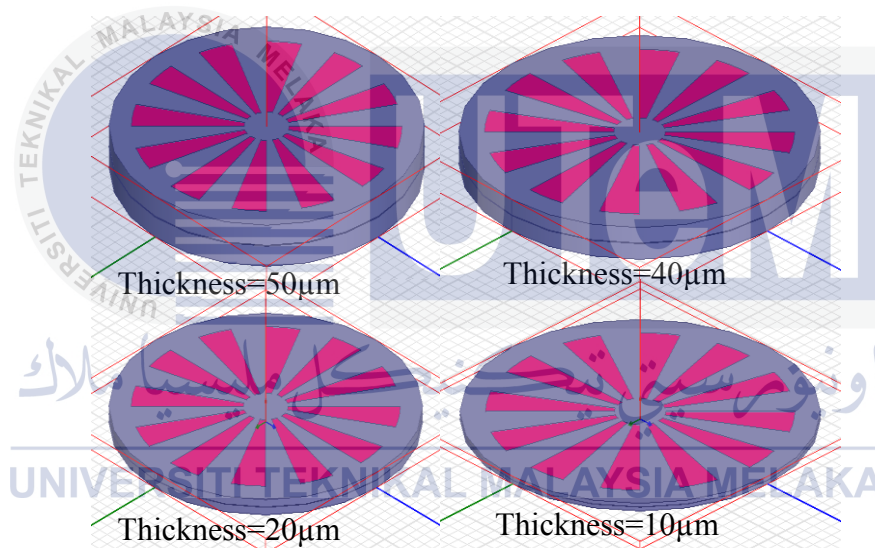


Figure 3.8: Thickness of bottom-drive actuator vary from 50 μm to 10 μm

3.5.3 Vary the teeth number of stator and rotor

To run this simulation, the number of teeth is manipulated, which mean the number of teeth activated per phase is varied. To vary the teeth number, the ratio of electrode to spacer, the gap between stator and rotor, the size of actuator, and the thickness of actuator has to be fixed; the only variables that are manipulating are

voltage supplied and the number of teeth. Figure 3.9 and Figure 3.10 show the actuators varied in different teeth ratio.

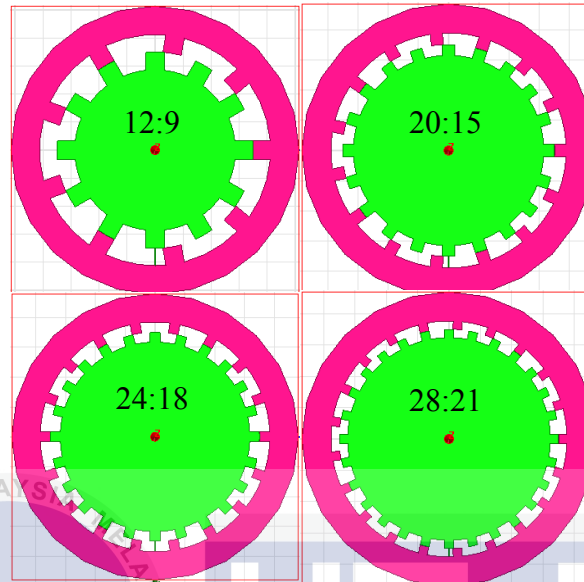


Figure 3.9: Teeth ratio of side-drive actuator vary from 12:9 to 28:21

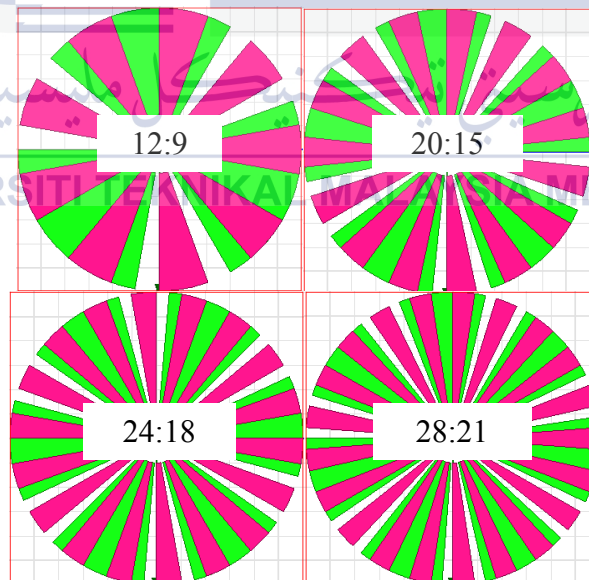


Figure 3.10: Teeth ratio of bottom-drive actuator vary from 12:9 to 28:21

CHAPTER 4

RESULT & DISCUSSION

4.1 Preliminary Results

4.1.1 Effect of electrode width and voltage on electrostatic force

Before start to do simulation, theoretical results are calculated using formula (3.1). Table 4.1 shows the force of Design 1 by fixing the value of distance between stator and rotor, $d = 2\ \mu m$ and manipulating the value of electrode width $10\ \mu m$ to $50\ \mu m$ and voltage from $0V$ to $100V$.

The relationship between width of rotor pole, voltage applied and force produced is shown in Figure 4.1 and Figure 4.2. From Figure 4.1 and Figure 4.2, as the width of rotor pole increases, the force increases linearly. This can be explained that as the width increases, the length that contact with electric field also increases, causing increment in the force. Same goes to voltage, as voltage applied increases, the force also increases exponentially. As the applied voltage increases, the electric field strength also increases, results in increment of force.

Table 4.1: Force of Design 1 by manipulating the electrode width and voltage

Width (μm)	Voltage (V)	Force (nN)
10	0	0
	10	8.85
	20	35.42
	30	79.69
	40	141.67
	50	221.35
	60	318.75
	70	433.86
	80	566.67
	90	717.19
	100	885.42
20	0	0
	10	17.71
	20	70.83
	30	159.38
	40	283.33
	50	442.71
	60	637.5
	70	867.71
	80	1133.34
	90	1434.38
	100	1770.84
30	0	0
	10	26.56
	20	106.25
	30	239.06
	40	425
	50	664.06
	60	956.25
	70	1301.57
	80	1700
	90	2151.57
	100	2656.26
40	0	0
	10	35.42
	20	141.67
	30	318.75

	40	566.67
	50	885.42
	60	1275
	70	1735.42
	80	2266.67
	90	2868.76
	100	3541.68
50	0	0
	10	44.27
	20	177.08
	30	398.44
	40	708.34
	50	1106.77
	60	1593.75
	70	2169.28
	80	2833.34
	90	3585.95
	100	4427.09

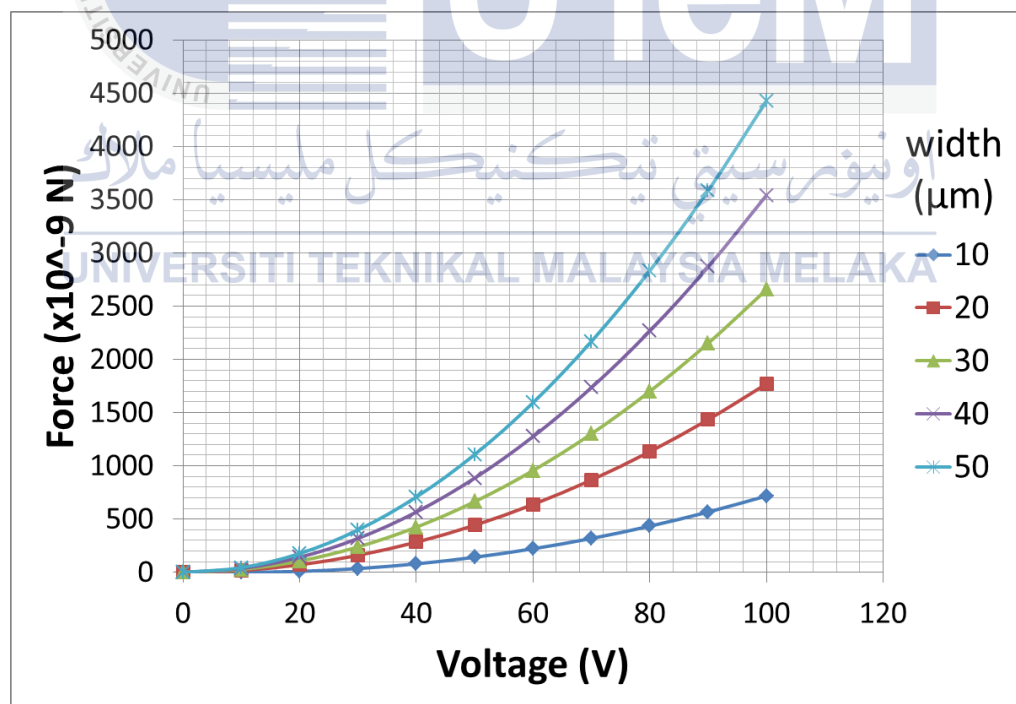


Figure 4.1: Force of Design 1 by manipulating electrode width and voltage

Same steps are applied to Design 2, Table 4.2 shows the electrostatic force of Design 2 by fixing the value of distance between stator and rotor, $d = 2\mu m$ and manipulating the value of electrode width from $100\mu m$ to $500\mu m$ and voltage from 0V to 100V.

Table 4.2: Force of Design 2 by manipulating the width and voltage

Width (μm)	Voltage (V)	Force (nN)
100	0	0
	10	88.54
	20	354.17
	30	796.88
	40	1416.67
	50	2213.55
	60	3187.51
	70	4338.55
	80	5666.68
	90	7171.89
	100	8854.19
200	0	0
	10	177.08
	20	708.34
	30	1593.75
	40	2833.34
	50	4427.09
	60	6375.02
	70	8677.1
	80	11333.36
	90	14343.78
	100	17708.38

300	0	0
	10	265.63
	20	1062.5
	30	2390.63
	40	4250.01
	50	6640.64
	60	9562.52
	70	13015.66
	80	17000.04
	90	21515.68
	100	26562.56
400	0	0
	10	354.17
	20	1416.67
	30	3187.51
	40	5666.68
	50	8854.19
	60	12750.03
	70	17354.21
	80	22666.72
	90	28687.57
	100	35416.75
500	0	0
	10	442.71
	20	1770.84
	30	3984.38
	40	7083.35
	50	11067.73
	60	15937.54
	70	21692.76
	80	28333.4
	90	35859.46
	100	44270.94

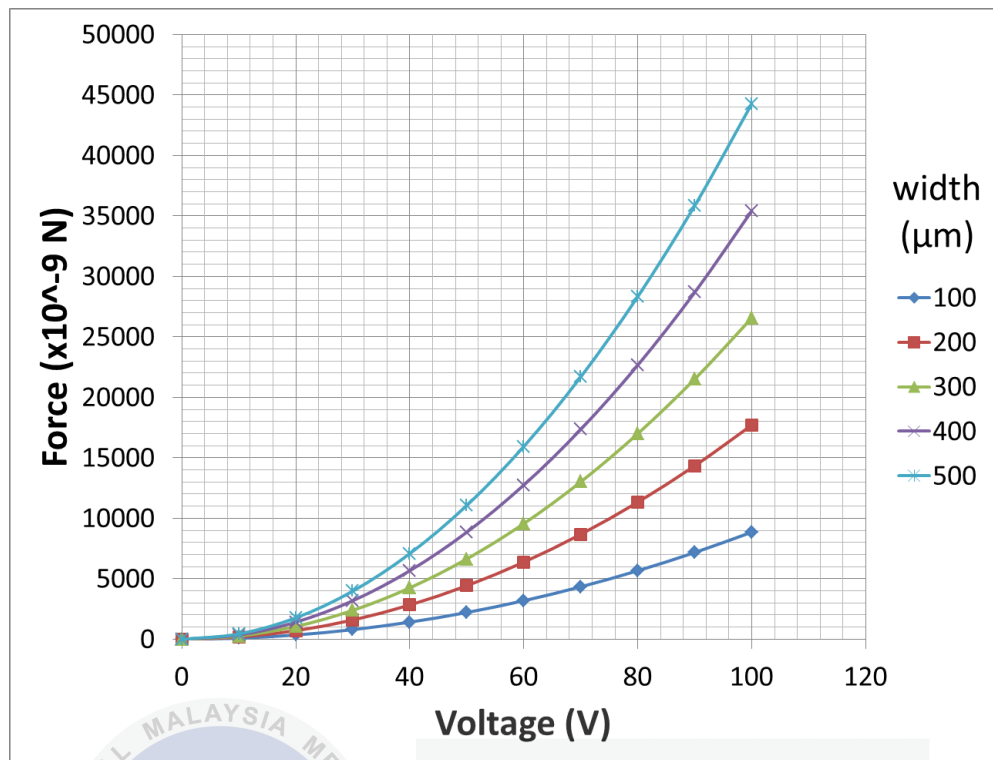


Figure 4.2: Force of Design 2 by manipulating electrode width and voltage

4.1.2 Effect of gap and voltage on electrostatic force

For the next calculation, the voltage and gap between stator and rotor are manipulated to find out the effect on electrostatic force. Table 4.3 shows the force of Design 1 by fixing the value of electrode width, $w = 50\mu m$ and manipulating the value of gap from $2\mu m$ to $5\mu m$ and voltage from 0V to 100V.

Based on Figure 4.3 and Figure 4.4, when the gap between stator and rotor increased, the electrostatic force however decreased. This is because when the distance between stator and rotor increases, the electric field strength will become weaker, causing the electrostatic force decreases.

Table 4.3: Force of Design 1 by manipulating gap and voltage

Gap (μm)	Voltage (V)	Force (nN)
2	0	0
	10	44.27
	20	177.08
	30	398.44
	40	708.34
	50	1106.77
	60	1593.75
	70	2169.28
	80	2833.34
	90	3585.95
	100	4427.09
3	0	0
	10	29.51
	20	118.06
	30	265.63
	40	472.22
	50	737.85
	60	1062.5
	70	1446.18
	80	1888.89
	90	2390.63
	100	2951.4
4	0	0
	10	22.13
	20	88.54
	30	199.22
	40	354.17
	50	553.39
	60	796.88
	70	1084.64
	80	1416.67
	90	1792.97
	100	2213.55

5	0	0
	10	17.71
	20	70.83
	30	159.38
	40	283.33
	50	442.71
	60	637.5
	70	867.71
	80	1133.34
	90	1434.38
	100	1770.84

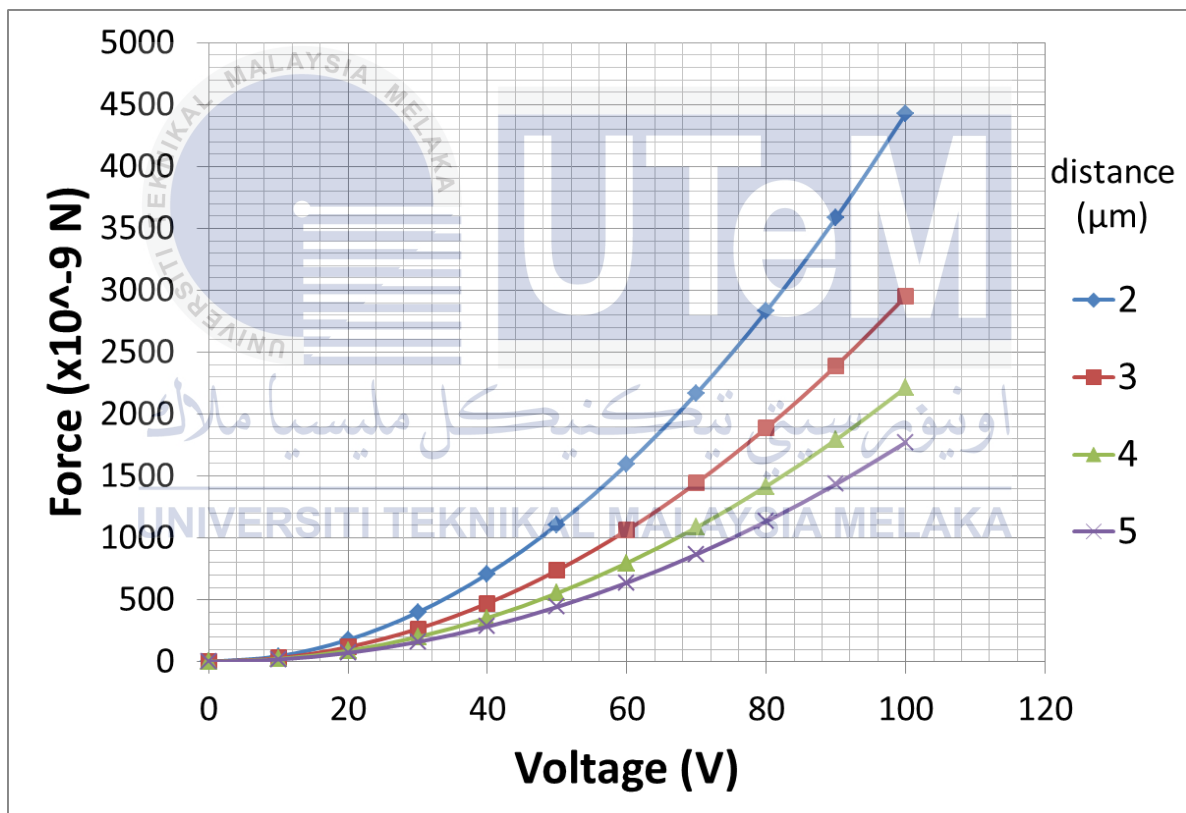


Figure 4.3: Force of Design 1 by manipulating gap and voltage

Table 4.4 shows the force of Design 2 by fixing the value of electrode width, $w = 500 \mu\text{m}$ and manipulating the value of gap from $2 \mu\text{m}$ to $5 \mu\text{m}$ and voltage from 0V to 100V.

Table 4.4: Force of Design 2 by manipulating gap and voltage

Gap (μm)	Voltage (V)	Force (nN)
2	0	0
	10	442.71
	20	1770.84
	30	3984.38
	40	7083.35
	50	11067.73
	60	15937.54
	70	21692.76
	80	28333.4
	90	35859.46
	100	44270.94
3	0	0
	10	295.14
	20	1180.56
	30	2656.26
	40	4722.23
	50	7378.49
	60	10625.03
	70	14461.84
	80	18888.93
	90	23906.31
	100	29513.96
4	0	0
	10	221.35
	20	885.42
	30	1992.19
	40	3541.68
	50	5533.87
	60	7968.77
	70	10846.38
	80	14166.7
	90	17929.73
	100	22135.47

5	0	0
	10	177.08
	20	708.34
	30	1593.75
	40	2833.34
	50	4427.09
	60	6375.02
	70	8677.1
	80	11333.36
	90	14343.78
	100	17708.38

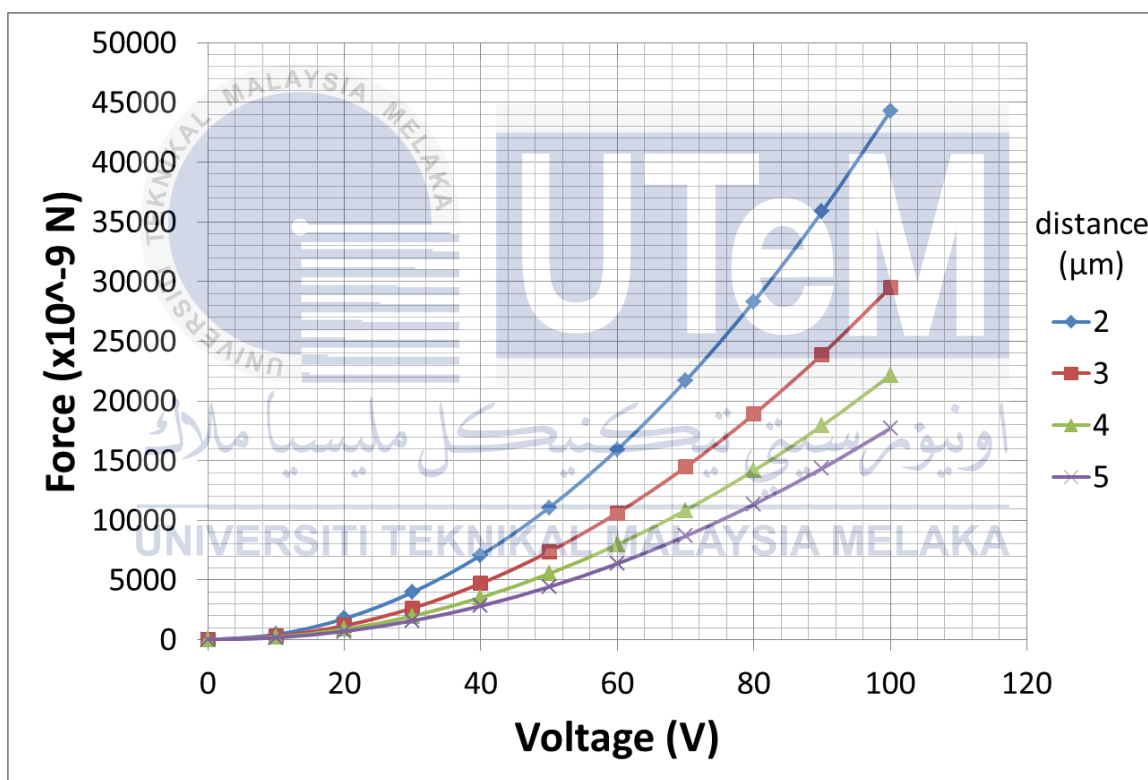


Figure 4.4: Force of Design 2 by manipulating gap and voltage

4.1.3 Effect of electrode width and gap on electrostatic force

To ensure the results obtained above, calculation by manipulating electrode width and gap is made. From the graphs show in Figure 4.5 and Figure 4.6, a conclusion can be made that by increasing the gap between stator and rotor and decreasing the width of electrode will weaken the electrostatic force. Table 4.5 shows the force of Design 1 by fixing the value of voltage, $V = 100V$ and manipulating the value of electrode width from $10\mu m$ to $50\mu m$ and gap from $2\mu m$ to $5\mu m$.

Table 4.5: Force of Design 1 by manipulating gap and electrode width

Gap (μm)	Width (μm)	Force (nN)
2	10	885.42
	15	1328.13
	20	1770.84
	25	2213.55
	30	2656.26
	35	3098.97
	40	3541.68
	45	3984.38
	50	4427.09
	50	4427.09
3	10	590.28
	15	885.42
	20	1180.56
	25	1475.7
	30	1770.84
	35	2065.98
	40	2361.12
	45	2656.26
	50	2951.4

4	10	442.71
	15	664.06
	20	885.42
	25	1106.77
	30	1328.13
	35	1549.48
	40	1770.84
	45	1992.19
	50	2213.55
5	10	354.17
	15	531.25
	20	708.34
	25	885.42
	30	1062.5
	35	1239.59
	40	1416.67
	45	1593.75
	50	1770.84

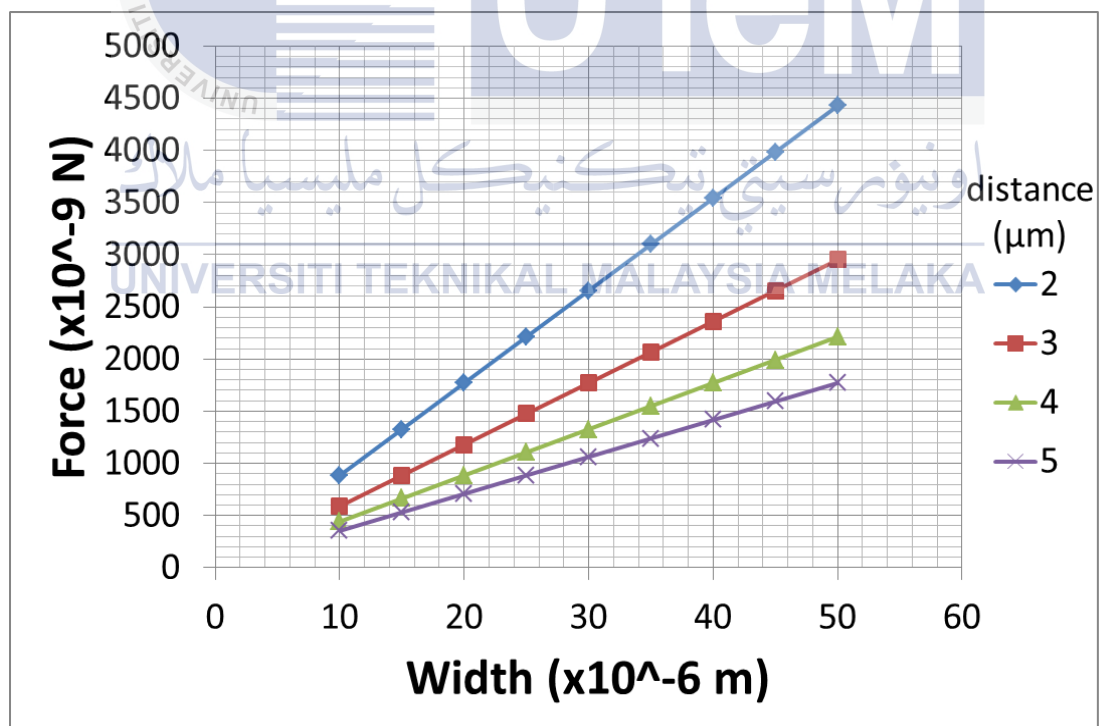


Figure 4.5: Force of Design 1 by manipulating electrode width and gap

Table 4.6 shows the force of Design 1 by fixing the value of voltage, $V = 100V$ and manipulating the value of electrode width and gap.

Table 4.6: Force of Design 2 by manipulating width and distance

Distance (μm)	Width (μm)	Force (nN)
2	100	8854.19
	150	13281.28
	200	17708.38
	250	22135.47
	300	26562.56
	350	30989.66
	400	35416.75
	450	39843.85
	500	44270.94
3	100	5902.79
	150	8854.19
	200	11805.58
	250	14756.98
	300	17708.38
	350	20659.77
	400	23611.17
	450	26562.56
	500	29513.96
4	100	4427.09
	150	6640.64
	200	8854.19
	250	11067.73
	300	13281.28
	350	15494.83
	400	17708.38
	450	19921.92
	500	22135.47

5	100	3541.68
	150	5312.51
	200	7083.335
	250	8854.19
	300	10625.03
	350	12395.86
	400	14166.7
	450	15937.54
	500	17708.38

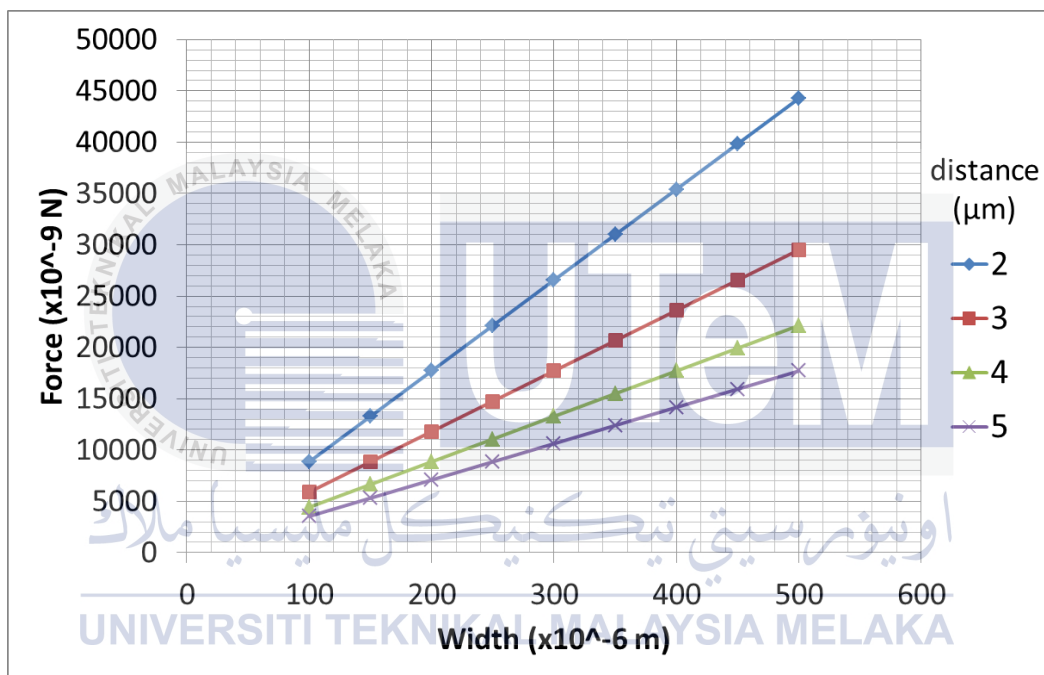


Figure 4.6: Force of Design 2 by manipulating width and distance

From the preliminary results, Design 2 shows the almost same results as Design 1, but with the force ten times greater than Design 1 because the electrode width of Design 2 is ten times wider than Design 1.

Finally the summary of the preliminary results is shown below. Table 4.7 shows the best parameters for both Design 1 and Design 2 after concluded from the results shown above.

Table 4.7: The best parameter for Design 1 and Design 2

Parameter	Design 1	Design 2
Voltage, V	100V	100V
Distance, d	2 μm	2 μm
Width, w	50 μm	500 μm

4.2 Simulation results

4.2.1 Effect of actuator size on electrostatic force

The relationship between size of actuator, voltage applied and electrostatic force produced are shown in Figure 4.7 and Figure 4.8. As the size of actuators decreased, the area overlapping of rotor and stator electrodes are also decreased, therefore we can conclude that electrostatic force depends on the area overlapping between stator and rotor electrodes. By comparing Figure 4.7 and Figure 4.8, the electrostatic force of bottom-drive actuator is higher than the electrostatic force of side-drive actuator because the area overlapping of bottom-drive actuator is larger than area overlapping of side-drive actuator.

UNIVERSITI TEKNIKAL MALAYSIA MELAKA

Table 4.8: Electrostatic force by varying side-drive actuator size

Rotor Radius (μm)	Voltage	Force (μN)
100	30V	0.049496
	60V	0.18642
	100V	0.9375
200	30V	0.38745
	60V	2.7286
	100V	13.655
300	30V	0.47126
	60V	2.321
	100V	6.9526

400	30V	1.9058
	60V	6.5932
	100V	25.257
500	30V	2.0991
	60V	9.1551
	100V	26.372
600	30V	1.2326
	60V	4.4706
	100V	13.444
700	30V	19.654
	60V	83.197
	100V	240.96

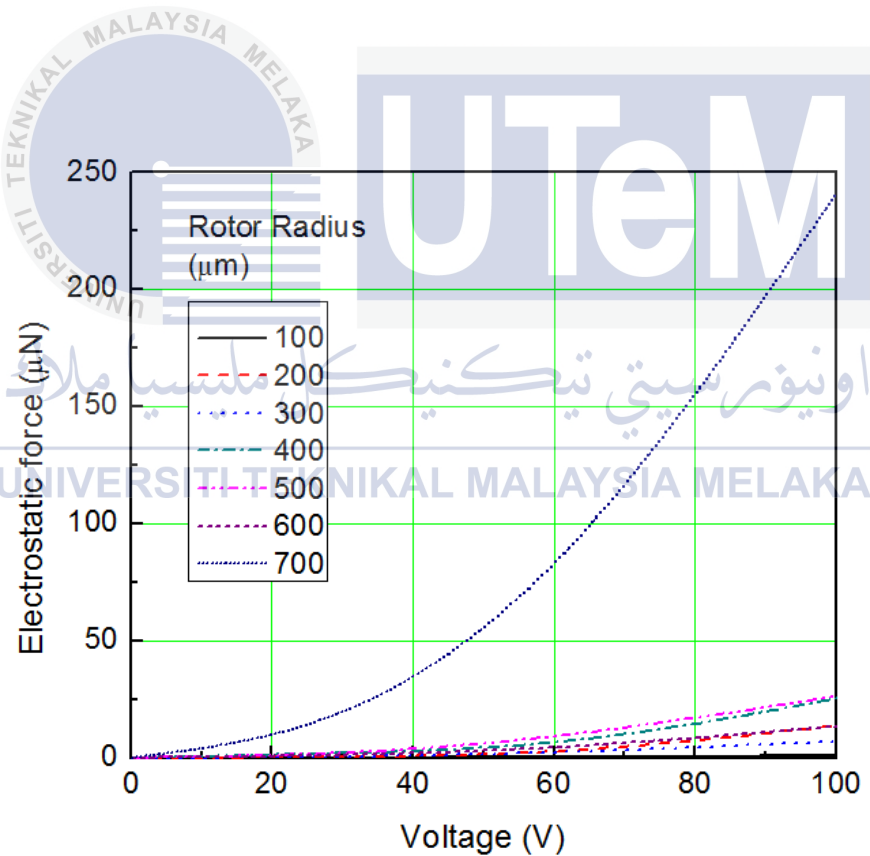


Figure 4.7: Electrostatic force produced with different side-drive actuator size. The measurements were performed with different voltages.

Table 4.9: Electrostatic force by varying bottom-drive actuator size

Rotor Radius (μm)	Voltage	Force (μN)
100	30V	10.843
	60V	43.697
	100V	122.81
200	30V	40.028
	60V	155.59
	100V	424.65
300	30V	83.715
	60V	344.45
	100V	989.16
400	30V	154.53
	60V	600.67
	100V	1620.3
500	30V	219.74
	60V	900.55
	100V	2575.3
600	30V	340.11
	60V	1315.3
	100V	3566.5
700	30V	421.64
	60V	1727.8
	100V	4931.8

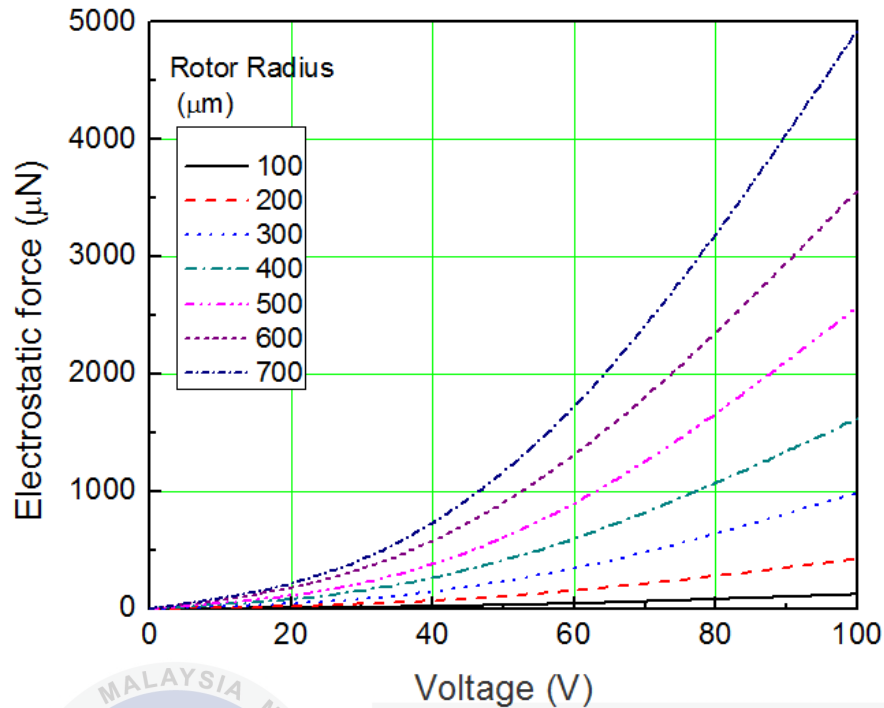


Figure 4.8: Electrostatic force produced with different bottom-drive actuator size. The measurements were performed with different voltages.

4.2.2 Effect of actuator thickness on electrostatic force

The effect of manipulating the actuator thickness is shown in Figure 4.9 and Figure 4.10. In Figure 4.9, changing the thickness of side-drive actuator does affect the electrostatic force produced because the area overlapping is depends on the thickness of the actuator. However, Figure 4.10 shows that changing the thickness of bottom-drive actuator does not affect the electrostatic force because the area overlapping of bottom-drive actuator does not depend on the thickness of actuator. By comparing two graphs, bottom-drive actuator produced greater electrostatic force than side-drive actuator although manipulating the thickness of actuator does not affect the electrostatic force.

Table 4.10: Electrostatic force by varying side-drive actuator thickness

Actuator Thickness (μm)	Voltage	Force (μN)
10	30V	0.33576
	60V	1.3826
	100V	2.0343
20	30V	0.20937
	60V	1.3531
	100V	6.2505
30	30V	4.467
	60V	16.618
	100V	38.758
40	30V	3.5842
	60V	13.644
	100V	44.3
50	30V	22.155
	60V	88.621
	100V	240.96

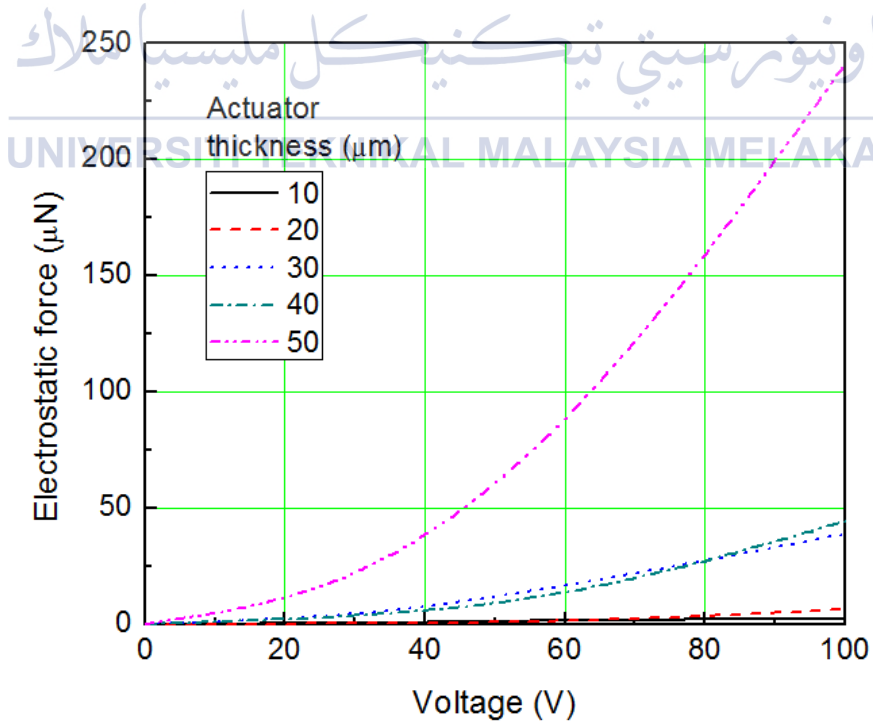


Figure 4.9: Electrostatic force produced with different side-drive actuator thickness.

Table 4.11: Electrostatic force by varying bottom-drive actuator thickness

Actuator Thickness (μm)	Voltage	Force (μN)
10	30V	443
	60V	1720.7
	100V	4663.9
20	30V	422.54
	60V	1728.2
	100V	4933.5
30	30V	450.24
	60V	1752.5
	100V	4769.6
40	30V	452.13
	60V	1763.7
	100V	4770.9
50	30V	421.64
	60V	1727.8
	100V	4931.8

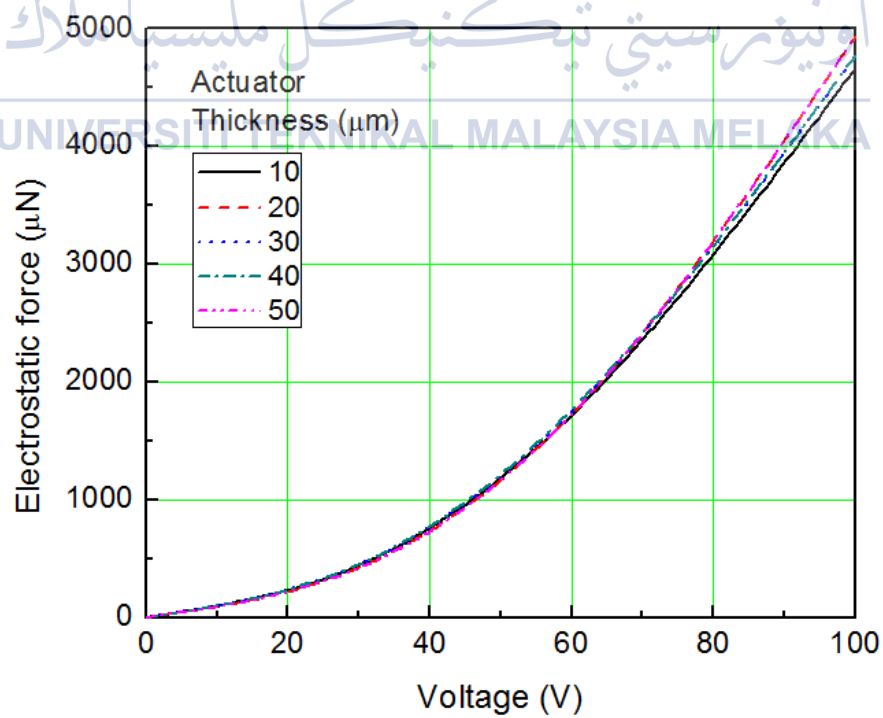


Figure 4.10: Electrostatic force produced with different bottom-drive actuator thickness.

4.2.3 Effect of teeth number on electrostatic force

From Figure 4.11 and Figure 4.12, the results show that most of the ratio has the almost the same electrostatic force, this is because when the number of teeth is increased, the area overlapping between stator electrode and rotor electrode will be decreased; but at the same time the distance travel per step input will be decreased too as well. When the area overlapping decreases, the electrostatic force decreases; when the distance travel per step decreases, the electrostatic force increases, or explain in another way, although the area overlapping will decreased when number of teeth is increased, but at the same time number of electrode activated per phase also increased. Therefore in this situation, the electrostatic force tends to remain the same when the number of teeth is varied.

Table 4.12: Electrostatic force produced by varying teeth ratio of side-drive actuator

Rotor to Stator Teeth Ratio	Voltage (V)	Force (μN)	Area Overlapping (μm^2)	Distance Travel Per Step (μm)
12:9	30	1.4476	6672.3	122.157
	60	5.3276		
	100	15.375		
16:12	30	22.155	5004.2	91.574
	60	88.621		
	100	240.96		
20:15	30	2.3028	4003.4	73.258
	60	7.0117		
	100	16.744		
24:18	30	2.7686	3336.2	61.057
	60	9.5996		
	100	26.164		
28:21	30	0.52269	2859.6	52.346
	60	1.5892		
	100	3.3536		

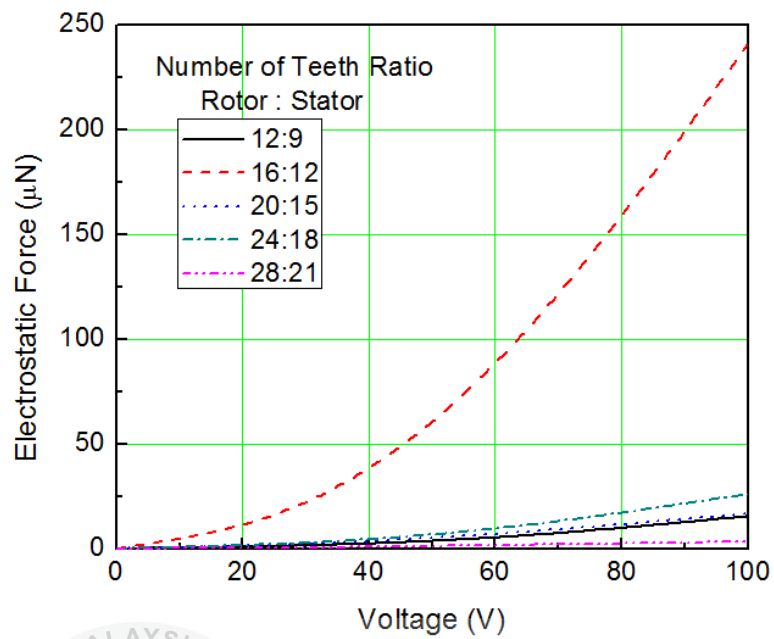


Figure 4.11: Electrostatic force produced with different side-drive actuator teeth number.

Table 4.13: Electrostatic force produced by varying teeth ratio of bottom-drive actuator

Rotor to Stator Teeth Ratio	Voltage (V)	Force (μN)	Area Overlapping (μm^2)	Distance Travel Per Step (μm)
12:9	30	412.02	61086.52	104.61
	60	1684.8		
	100	4811.2		
16:12	30	421.64	45814.89	78.51
	60	1727.8		
	100	4931.8		
20:15	30	442.37	36651.91	62.83
	60	1820.8		
	100	5209.6		
24:18	30	452.88	30543.26	52.38
	60	1862.6		
	100	5346.4		

28:21	30	468.94	26179.94	44.91
	60	1939.4		
	100	5587.4		

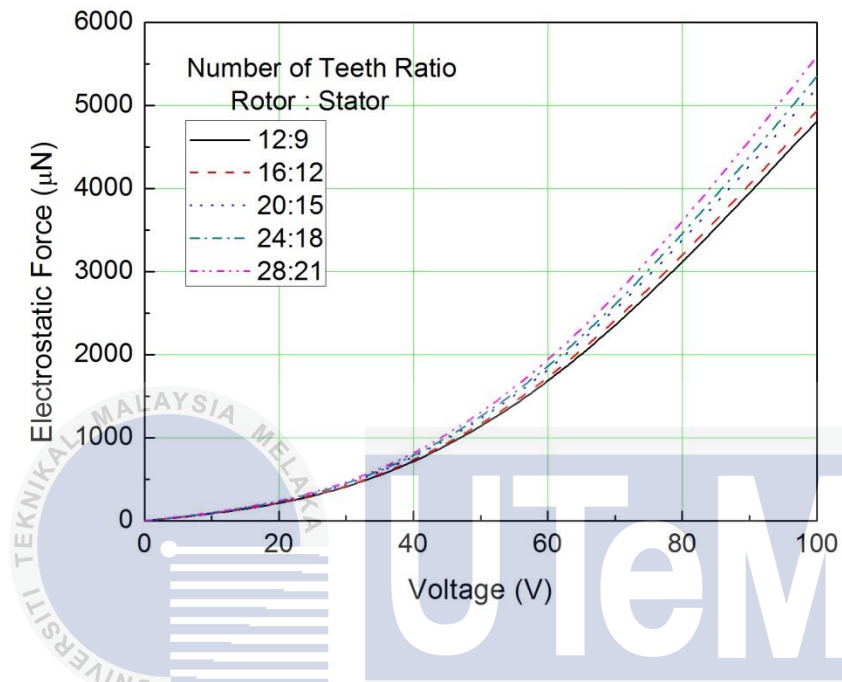


Figure 4.12: Electrostatic force produced with different bottom-drive actuator teeth number.

اونيورسيتي تيكنيكل مليسيا ملاك

UNIVERSITI TEKNIKAL MALAYSIA MELAKA

CHAPTER 5

CONCLUSION

The pros and cons of different microactuators are compared in the beginning. Electrostatic actuator is selected due to its small size scale and also other advantages stated. Rotary motion electrostatic actuator is chosen because it allows higher speed of actuation, higher efficiency, and longer working range. Both designs are three-phase variable-capacitance actuators with the same rotor size (radius, $r = 700\ \mu\text{m}$), same number of rotor electrodes (16 electrodes) and stator electrodes (12 electrodes). The best parameters for both designs are selected from the results. From the early results, Design 2 (bottom-drive electrostatic actuator) is theoretically better than Design 1 (side-drive electrostatic actuator), but further simulations are needed to find out the best design for rotary motion electrostatic actuator. Therefore Finite Element Method (FEM) is used to analyse both designs because it is a very powerful numerical tool in simulation and analysis of all virtual engineering problems. Three simulations have been carried out; first, vary the actuator size; second, vary the actuator thickness; third, vary the number of electrode. With the same rotor size, thickness, gap, and number of electrode, the simulation results show that bottom-drive electrostatic actuator has better performance than side-drive electrostatic actuator.

REFERENCES

- [1] X. Wang, S. Cui, and S. Cheng, "Advantages of electrostatic micromotor and its application to medical instruments," presented at Conference Record of the 2002 IEEE Industry Applications, Pittsburgh, PA, USA, 2002.
- [2] D. Polla, A. Erdman, D. Peichel, R. Rizq, Y. Gao, and D. Markus, "Precision micromotor for surgery," presented at Proceedings of 1st Annual International IEEE-EMBS Special Topic Conference on Microtechnologies in Medicine and Biology, Lyon, France, 12-14 Oct. 2000.
- [3] L. M. Gao, Y. Chen, L. M. Lin, and G. Z. Yan, "Micro motor based new type of endoscope," presented at Proceedings of the 20th Engineering in Medicine and Biology Society, Hong Kong, China, 1998.
- [4] W. S. N. Trimmer and K. J. Gabriel, "Design Consideration for a Practical Electrostatic Micro-motor," *Sensors and Actuators*, vol. 11, pp. 189-206, 1987.
- [5] O. D. Jefimenko and D. K. Walker, *Electrostatic motors: their history, types, and principles of operation*. Star City, West Virginia: Electret Scientific Company, 1973.
- [6] Ch. A. Coulomb, "Recherches théoriques et expérimentales sur la force de torsion et sur l'élasticité des fils de metal", *Histoire de l'Académie Royale des Sciences*, 229-269, Paris, 1784
- [7] Ch. A. Coulomb, *Premier Mémoire sur l'Electricité et le Magnétisme*, *Histoire de l'Académie Royale des Sciences*, 569-577, Paris, 1785.

- [8] M. Karpelson, G.-Y. Wei, and R. J. Wood, "A review of actuation and power electronics options for flapping-wing robotic insects," *IEEE International Conference on Robotics and Automation*, Pasadena, CA, USA, pp. 779-786, May 2008.
- [9] E. Sarajlic, C. Yamahata, M. Cordero, L. Jalabert, T. Iizuka, H. Fujita, "Single Mask 3- Phase Electrostatic Rotary Stepper Micromotor", in *Proc. 15*
- [10] W. S. N. Trimmer and K. J. Gabriel, "Design considerations for a practical electrostatic micro-motor," *Sens. Actuators*, vol. 11, no. 2, pp. 189–206, Mar. 1987.
- [11] W. C. Tang, T. C. H. Nguyen, and R. T. Howe, "Laterally driven polysilicon resonant microstructures," in *Proc. Micro Electro Mechanical Systems*, 1989, pp. 53-59.
- [12] P. B. Chu, P. R. Nelson, M. L. Tachiki, and K. S. J. Pister, "Dynamics of polysilicon parallel-plate electrostatic actuators," *Sensors and Actuators A*, vol. 52, no. 1-3, pp. 216–220, March 1996.
- [13] H. S. Carslaw and J. C. Jaeger, *Conduction of Heat in Solids*. Oxford University Press, 1986.
- [14] S. Prasanna and S. M. Spearing, "Materials selection and design of microelectrothermal bimaterial actuators," *J. of Microelectromechanical Systems*, vol. 16, no. 2, pp. 248–259, April 2007.
- [15] Q. M. Wang and L. E. Cross, "Performance analysis of piezoelectric cantilever bending actuators," *Ferroelectrics*, vol. 215, no. 1-4, pp. 187–213, 1998.
- [16] D. R. Madill and D. Wang, "Modelling and L2-stability of a shape memory alloy position control system," *IEEE Trans. on Control Systems Technology*, vol. 6, no. 4, pp. 473–481, July 1998.
- [17] P. Krulevitch, *et al.*, "Thin film shape memory alloy microactuators," *J. of Microelectromechanical Systems*, vol. 5, no. 4, pp. 270–282, 1996.
- [18] R. D. Kornbluh, *et al.*, "Electroelastomers: Applications of dielectric elastomer transducers for actuation, generation, and smart structures," in *Proc. SPIE*, vol. 4698, 2002, pp. 254–270.

- [19] P. Dario, R. Valleggi, M.C. Carrozza, M.C. Montesi, and M. Cocco, "Microactuators for microrobotics: a critical survey", *Journal of Micromechanics and Microengineering*, 1992, Vol.2, No.3, pp141-157



APPENDIX A

GANTT CHART

	2013				2014					
Project Activities	Sept.	Oct.	Nov.	Dec.	Jan.	Feb.	Mar.	Apr.	May	Jun.
Research and study topic										
Draft out design and proposal										
Conduct experiment and collect data										
Report preparation and presentation										
Model building (software)										
Analysis on design performance										
Final presentation										